

Flux-Pinning Behaviors and Mechanism According to Dopant Level in (Fe, Ti) Particle-Doped MgB₂ Superconductor

H. B. Lee,* G. C. Kim, Young Jin Shon, Dongjin Kim, and Y. C. Kim

Department of Physics, Pusan National University, Busan 46241, Korea

Abstract

We have studied flux-pinning effects of MgB₂ superconductor by doping (Fe, Ti) particles of which radius is 163 nm on average. 5 wt.% (Fe, Ti) doped MgB₂ among the specimens showed the best field dependence of magnetization and 25 wt.% one did the worst at 5 K. The difference of field dependence of magnetization of the two increased as temperature increased. Here we show experimental results of (Fe, Ti) particle-doped MgB₂ according to dopant level and the causes of the behaviors. Flux-pinning effect of volume defects-doped superconductor was modeled in ideal state. During the study, we had to divide M-H curve of volume defect-dominating superconductor as three discrete regions for analyzing flux pinning effects, which are diamagnetic increase region, $\Delta H = \Delta B$ region, and diamagnetic decrease region. As a result, flux-pinning effects of volume defects decreased as dopant level increased over the optimal dopant level, which was caused by decrease of flux-pinning limit of a volume defect. And similar behaviors are obtained as dopant level decreased below the optimal dopant level, which was caused by the decreased number of volume defects. Comparing the theory with experimental results, deviations increased as dopant level increased over the optimal dopant level, whereas the two were well matched on less dopant level than the optimal dopant level. The behavior is considered to be caused by segregation of volume defects. On the other hand, the property of over-doped specimens dramatically decreases as temperature increases, which is caused by double decreases of flux-pinning limit of a volume defect and segregation effect.

*Electronic address: superpig@pusan.ac.kr; Fax: +82-51-513-7664

I. INTRODUCTION

We have studied the flux-pinning effects of MgB₂ superconductor by doping (Fe, Ti) particles of which radius is 163 nm on average [1–3]. Investigating field dependences of magnetization (FDM) of the doped MgB₂ specimens, 5 wt.% doped specimen showed the best FDM and FDMs of other doped specimen became poorer as dopant level increases or decreases. The behavior means that there was the optimal dopant level for the best FDM when MgB₂ were doped with the (Fe, Ti) particles. Although the behaviors might be interesting enough, the exact mechanism has not been revealed.

On the other hand, there were several reports that diamagnetic property and critical current (J_c) were changed according to dopant level [4–8]. However, detailed mechanism and the cause have been not shown. According to our studies, one thing to note is that the optimal concentration of defects for best performance depended on the state of pinning sites that defects produced []. For example, flux-pinning effects of defects depended on which types, what sizes, and how many.

The conventional theory for ideal type II superconductor represented two critical fields which are lower critical field (H_{c1}) and upper critical field (H_{c2}) in field dependence of magnetization curve (M-H curve) as shown Fig. 1 (a) [9, 10]. However, M-H curves of current specimens, which are one of volume defect-dominating superconductors, showed quite different behavior from that of ideal superconductor [11–16]. Thus, we have to explain M-H curves by dividing them into three discreet regions as shown Fig. 1 (b). The first is the diamagnetic property increase region (region I), the second is $\Delta H = \Delta B$ region (region II), and the third is the diamagnetic decrease region (region III). The cause of the distinction is that M-H curves of real superconductors are heavily influenced by flux-pinning phenomena of defects and each region has different mechanism [2, 3].

Regarding the region of diamagnetic increase (region I), pinned fluxes at a volume defect are picked out (pick-out depinning) from the defect when $F_{pickout}$ is larger than $F_{pinning}$. The basis of diamagnetic increase after H_{c1} is that the magnetic fluxes have penetrated into the superconductor after H_{c1} are pinned at volume defects. Thus, they would be another barrier to prevent the fluxes penetrating into the superconductor if they are pinned at volume defects.

In $\Delta H = \Delta B$ region (region II), a different cause is applied to the movement of pinned

fluxes at volume defects. The shortest distance between pinned fluxes at volume defects would determine whether the pinned fluxes have to be pick-out depinned or not. Thus they could be pick-out depinned and move although $F_{pickout}$ is smaller than $F_{pinning}$ [17]. Pick-out depinning was named by the behavior of depinning that pinned fluxes are picked out together when they are depinned from the volume defect. The behavior of pinned fluxes in $\Delta H = \Delta B$ region are influenced by the nature that neighborhoods of a volume defect would lose superconductivity if the shortest distance between pinned fluxes at the volume defect is the same as that of H_{c2} . Thus, flux-pinning itself is not established in the state and pinned fluxes at a volume defect are pick-out depinned although $F_{pickout}$ is smaller than $F_{pinning}$.

Regarding the diamagnetic decrease region (region III), it is the region that flux-pinning effect of volume defects decreases. In the region, magnetic fluxes which are not pinned at volume defects increase as applied magnetic field increases and the increase of unpinned fluxes results in a decrease of diamagnetic property of the superconductor by $4\pi M = B - H$, where M , B and H are magnetization, magnetic induction, and applied magnetic field, respectively. The difference between conventional theory of ideal superconductor after H_{c1} and region III of the current representation is the decrease rate of diamagnetic property. The decrease rate was smaller as applied magnetic field increases when flux-pinning effects of volume defects increased (i.e. $\Delta H = \Delta B$ region is wider).

One may ask "It is natural that flux-pinning effects of volume defects decrease if a dopant level increases because ΔG_{defect} is shallowed, which are caused by decreased portion of superconductivity." However, the concept is considered to be came from the conventional view of superconductors. According to the concept of superconductor, ΔG_{defect} of 1 wt.% doped MgB_2 and pure MgB_2 must have deeper ΔG_{defect} than those of higher dopant level specimens. However, the results of current experiments are too far from it, which is 5 wt.% doped MgB_2 showed deepest ΔG_{defect} in wider applied magnetic field. The basis of ΔG_{defect} is the field that represents the diamagnetic property ($\Delta G_{defect} = -\frac{(H-B)^2}{8\pi} \times \frac{4}{3}\pi r^3$, where H is applied magnetic field and B is magnetic induction). Depending on kinds of volume defects, ΔG_{defect} could be deeper if flux-pinning effect of the volume defects were good. And ΔG_{defect} could be shallower if flux-pinning effects of volume defects were poor. Therefore, it is not reasonable that the increased number of volume defects caused ΔG_{defect} to be shallower.

In this paper, we would study the cause of the best field dependence of magnetization of 5 wt.% (Fe, Ti) doped MgB_2 specimen and the cause of gradual decreases of field dependence

of magnetization in other dopant level of MgB₂ specimens as dopant level decreases or increases from the 5 wt.%.

II. RESULTS

A. Experimental results of field dependences of magnetization for (Fe, Ti) particle-doped MgB₂ specimens

Figure 2 (a) shows M-H curves of (Fe, Ti) particle-doped MgB₂ specimens at 5 K according to dopant level, which are doped with (Fe, Ti) particles of which radius are 163 nm on average. Inspecting region I, maximum diamagnetic properties (MDP) of the specimens except pure MgB₂ are almost same. However, they show different widths of region II, and 5 wt.% doped specimens showed the widest $\Delta H = \Delta B$ region. A width of the region is ordered as follows, 5% > 10% > 1% > 25% > pure. Pure MgB₂ has no $\Delta H = \Delta B$ region.

Inspecting the behaviors after $\Delta H = \Delta B$ region (region III) in M-H curves as shown in the figure, the decrease rate of diamagnetic property along applied magnetic field was lower as the width of the region was wider. After 5 wt.% doped specimen showed the lowest decrease rate of field dependence of magnetization (FDM) along applied magnetic field, decrease rates of other doped specimens increase as dopant level increases from 5 wt.%. And less doped specimens than 5 wt.% also showed same behaviors as dopant level decreases from 5 wt.%.

M-H curves of doped MgB₂ specimens at 30 K are shown in Fig. 3, which is results of the same specimens as shown in Fig. 2. At the temperature, flux-pinning effects of a superconductor have to be determined by heights of the maximum diamagnetic property (MDP) and the degree of diamagnetic decrease because $\Delta H = \Delta B$ region completely disappeared at 30 K. The specimen showing the best maximum diamagnetic property at 30 K is still 5 wt.% specimen, which had widest $\Delta H = \Delta B$ region at 5 K. However, other specimens have some changes on M-H curves. The MDP of 10 wt.% doped specimen is the next, which is same order when compared with a width of $\Delta H = \Delta B$ region at 5 K, but it is much closer to that of 1 wt.% doped specimen.

The figure also shows that a difference of diamagnetic decrease between 5 wt.% doped specimen and other specimens at 30 K much more increased when compared with those at 5 K. A noting thing is that 25 wt.% doped specimen showed much poorer diamagnetic

decrease at 30 K compared with that of pure MgB₂, which is reversed results at 5 K. From the considerations, it is understood that a degree of diamagnetic decrease at 30 K increases as dopant level increases from 5 wt.% doped specimen.

Considering the experimental results, it is needed to understand why 5 wt.% specimen at 5 K showed the optimal flux-pinning effects, why gradual decrease of a width of $\Delta H = \Delta B$ region occurred as the amount of dopant level increases or decreases from optimal dopant level, why a difference of diamagnetic decrease between the optimal flux-pinning specimen and other doped specimens significantly increase when the temperature increases at 30 K, and why superconducting properties of doped specimens go much poorer at 30 K as dopant level increases.

B. A representation of flux-pinning effect in ideal doped state

Figure 4 (a) shows a schematic representation of volume defect-doped superconductor. It is assumed that spherical volume defects of which radius is r are doped in cubic superconductor of which a length is D . Figure 4 (b) shows a schematic representation which is several quantum fluxes that are pinned together at volume defects. The shortest distance between pinned fluxes is d' and the widest one is d . Generally, the number of quantum fluxes (n^2) which can be pinned at a spherical volume defect are calculated as follows.

$$n^2 = \frac{\pi r^2}{d'^2} \quad (1)$$

where r and d' are radius of volume defect and the shortest distance between quantum fluxes pinned at the volume defect of which radius is r when they have square structure, respectively [3]. If d'^2 is $2\pi\xi^2$ (ξ is coherence length of the superconductor), a volume defect pin the maximum flux quanta, which is flux-pinning limit of a volume defect.

On the other hand, average d , which is average value of widest distance between pinned fluxes is

$$\bar{d} = \frac{D - r}{n} \quad (2)$$

where d , D , r , and n are the widest distance between pinned fluxes, a distance between volume defects, radius of volume defect, and the number of quantum fluxes pinned at volume defects in one dimension (1 D) in the state that they are arrayed in a row to the next volume defect as shown in Fig. 4 (b).

On the other hand, concerning the widest distance between pinned fluxes (d), minimum distance must be needed for flux-pinning effect of volume defects, and the reasons are as follows. The first is that forefront fluxes among pinned fluxes have more tension, thus the foremost d among pinned fluxes at volume defects (Fig. 4 (b)) must be shorter than average d . And the second is that pinned fluxes are affected by depinnings of other part of fluxes from neighborhood volume defects because pinned fluxes are interconnected from a volume defect to the next. Thus, pinned fluxes are vibrating if they are not depinned when other part of fluxes are depinned. The third is that they are affected by heat caused by depinning of other fluxes and other part of fluxes. Therefore, they cannot maintain flux-pinning state if the distance between pinned fluxes are shorter than the minimum distance, which must be much wider than that of H_{c2} .

The quantum flux pinned at volume defects would be divided into two parts, which are volume defect part and superconducting part as shown in Fig. 4 (b). Since quantum fluxes of volume defect part are fixed on the volume defects, they can withstand until the distance between them is same as that of H_{c2} because $F_{pinning}$ (the pinning force) of 163 nm radius volume defect is much larger than $F_{pickout}$ (the pick-out depinning force) in $\Delta H = \Delta B$ region [17]. However, quantum fluxes of superconducting part are less arrested on the volume defects because they are elastic and away from the volume defects. Therefore, they are highly affected by other fluxes movements and movements of other parts of quantum fluxes because a quantum flux is simultaneously pinned at 8000 volume defects in 5 wt.% doped MgB_2 , which result in that superconductivity of the part would disappear if the distance between the flux quanta were shorter than that of H_{c2} at any moment by the effects of environment.

Quantum state of magnetic fluxes would be maintained by the repulsive force generated by superconducting eddy currents, and pinned fluxes at volume defect are constantly influenced by the movement of other parts of pinned fluxes [9]. If quantum fluxes failed to be separated by the influence of other fluxes, the superconductivity of the part would disappear at the moment that the distance between fluxes is shorter than that of H_{c2} . The electrons that generate the magnetic flux would be not superconducting electrons anymore, which are Cooper pair. In order for normal electrons to generate magnetic fluxes, it is certain that many electrons have to participate.

Therefore, the heat caused by electric resistance would happen. If the generated heat

was small, it does not affect neighborhoods of quantum fluxes to combine, thus they would retain their superconductivity again. However, if it was large enough, it would affect the neighborhoods of quantum fluxes to combine because coherence length of a superconductor increases as temperature increases. Thus, the heat would propagate around it and causes other quantum fluxes to combine into one, which means that they are not a quantum flux anymore. At last, the entire pinned fluxes at volume defect become non-superconducting state. Thus, flux-pinning effects would disappear, and the pinned fluxes naturally are pick-out depinned from the defect. Therefore, some distance (d) between pinned fluxes at volume defects must be required to maintain superconductivity of pinned fluxes at a volume defect.

Therefore, flux-pinning limit of a volume defects at over-dopant level is

$$n_{ov}^2 = n_o^2 \left(\frac{D_{ov} - r}{D_o - r} \right)^2 \quad (3)$$

where n_o^2 , D_o , and D_{ov} are the number of pinned fluxes on a volume defect at optimal dopant level at 0 K, the distance between volume defects at optimal dopant level, and the distance between volume defects at over-dopant level, respectively. It was assumed that pinned fluxes at a volume are arrayed vertically equal.

And a rate of increased pinning sites by over-doping is

$$R = \frac{m_{ov}^2}{m_o^2} \quad (4)$$

where m_o^3 is the number of volume defects at optimal dopant level and m_{ov}^3 is the number of volume defects at over-dopant level. The equation was described because single flux quantum is pinned on volume defects along an axis. Therefore, total flux-pinning effects of volume defects at over-dopant level, which is expressed as a width of $\Delta H = \Delta B$ region, is

$$W_{\Delta H = \Delta B, ov} = \frac{n_{ov}^2}{n_o^2} \frac{m_{ov}^2}{m_o^2} W_{\Delta H = \Delta B, o} = \left(\frac{D_{ov} - r}{D_o - r} \right)^2 \frac{m_{ov}^2}{m_o^2} W_{\Delta H = \Delta B, o} \quad (5)$$

where $W_{\Delta H = \Delta B, ov}$ and $W_{\Delta H = \Delta B, o}$ are a width of $\Delta H = \Delta B$ region of over-dopant level and that of optimum level at 0 K, respectively.

On the other hand, under the state that volume defects are in less-dopant level, flux-pinning effects of the superconductor depend on the number of volume defects because flux-pinning limit of a volume defect is the same as that of optimum level.

$$W_{\Delta H = \Delta B, le} = \frac{m_{le}^2}{m_o^2} W_{\Delta H = \Delta B, o} \quad (6)$$

where $W_{\Delta H=\Delta B,le}$ is a width of $\Delta H=\Delta B$ region of less-dopant level and m_{le}^3 is the number of volume defects at less-dopant level in a superconductor.

Numerically, 5 wt.% (Fe, Ti) particles in MgB_2 approximately corresponds to 2.0 vol.% and D is $5.94r$. On the other hand, 25 wt.% (Fe, Ti) particles in MgB_2 corresponds to approximately 10 vol.% and D is $3.47r$. A spherical volume defect of 163 nm radius in 5 wt.% (Fe, Ti) particles-doped MgB_2 can pin approximately 51^2 flux quanta when H_{c2} is 65.4 Tesla (T) at 0 K [3]. Assuming that 51 quantum fluxes are arrayed in a row to the next volume defect, $\bar{d}_{5wt. \%}$ is 15.8 nm.

Table I shows various properties of (Fe, Ti)-doped MgB_2 specimens according to dopant level. $\bar{d}_{25wt. \%}$ is 7.89 nm for 25 wt.% (Fe, Ti)-doped MgB_2 if 51^2 flux quanta are pinned at 163 nm radius volume defect. Superconducting state would be destroyed if d is less than 5.63 nm when H_{c2} is 65.4 T at 0 K. Since the front d in pinned fluxes would be shorter than \bar{d} and the environments would affect d , it is certain that 163 nm radius volume defect cannot pin 51^2 flux quanta in dynamic state.

5 wt.% doped specimen showed the best flux-pinning effect, and of which $\bar{d}_{5wt. \%}$ is 15.8 nm as mentioned. The number of pinned fluxes (n^2) at 163 nm radius defect would be approximately 26^2 in 25 wt.% doped specimen if $\bar{d}_{5wt. \%}$ is set as the minimal distance. The calculation means that 163 nm radius volume defect of 25 wt.% doped specimen can pin up to only 26^2 flux quanta. Therefore, it is considered that the flux-pinning effect of a volume defect in 25 wt.% doped specimen decreases to 0.26 ($26^2/51^2$) by Eq. (3).

On the other hand, increased pinning sites of 25 wt.% doped specimen is 2.92 ($13680^2/8000^2$) by Eq. (4) because single flux quantum is pinned on 13680 volume defects per unit length (cm) along an axis. Thus, actual rate of flux-pinning effect by increased volume defects for 25 wt.% doped specimen are 0.75 (0.26×2.92) by Eq. (5). Table I also shows actual flux-pinning effect of increased volume defects for 10 wt.% doped specimen, which is 0.91. On the other hand, decreased flux-pinning effect of 1 wt.% specimen is 0.37 ($4860^2/8000^2$) by Eq. (6).

Comparing theoretical values with the experimental results as shown in Table I, $\Delta H=\Delta B$ region widths of 5 wt.%, 10 wt.%, 25 wt.%, and 1 wt.% are experimentally 1.5 Tesla (T), 1.0 T, 0.5 T, and 0.6 T, respectively, as shown Fig. 3 [18]. 1 wt.% specimen shows a good match with theoretical value ($0.6 \text{ T}/1.5 \text{ T} = 0.4$). However, as the dopant level increases from 5 wt.%, a difference between the experimental results and the calculation increases (10

wt.% specimen: $0.91 - 0.67 = 0.23$, 25 wt.% specimen: $0.75 - 0.33 = 0.42$). This means that there would be other factors decreasing flux-pinning effect in over-doped specimens.

C. The segregation effect of volume defects and temperature dependence of a width of $\Delta H = \Delta B$ region at over-dopant level

As the number of doped volume defects increases in a superconductor, average distance between them do not only decrease, but volume defects which are closer than average distance also increase. As discussed earlier, the shorter the distance between volume defects is, the fewer the pinning limit of a volume defect is. Furthermore, if the distance between them is shorter than $\sqrt{2\pi}\xi$ of the superconductor, they are recognized as a pinning site. Thus, the volume defects look like being connected each other in the state. Therefore, the fluxes move more easier along the volume defects. Consequently, the fluxes can quickly penetrate into an inside of the superconductor when applied field increases because the segregated volume defects have lower pinning limits.

The flux-pinning limit of a volume defect decreases as temperature increases, which is caused by increase of coherence length as temperature increases. Therefore, a width of $\Delta H = \Delta B$ region of optimal dopant level at a temperature is

$$W_{\Delta H = \Delta B(T),o} = \frac{n_T^2}{n_o^2} W_{\Delta H = \Delta B(0),o} \quad (7)$$

where n_T^2 is flux-pinning limit of a volume defect at a temperature and $W_{\Delta H = \Delta B,o}$ is a width of $\Delta H = \Delta B$ region of optimal level at 0 K.

In the state of over-dopant level, a width of $\Delta H = \Delta B$ region of at a temperature is

$$W_{\Delta H = \Delta B(T),ov} = \frac{n_{ov(T)}^2}{n_{ov(0)}^2} W_{\Delta H = \Delta B(0),ov} \quad (8)$$

On the other hand, as temperature increases, over-doped superconductor would have much lower flux-pinning effect because volume defects have two kinds of decreases of flux-pinning limits. One is a decrease of flux-pinning limit of a volume defect by over-doping, and the other is that of temperature increase, the two both are caused by increase of coherence length as temperature increases. Therefore,

$$W_{\Delta H = \Delta B(T),ov} = \frac{n_{ov(T)}^2}{n_{ov(0)}^2} W_{\Delta H = \Delta B(0),ov} = \frac{n_{ov(T)}^2}{n_{ov(0)}^2} \frac{n_{ov}^2}{n_o^2} \frac{m_{ov}^2}{m_o^2} W_{\Delta H = \Delta B(0),o} \quad (9)$$

where n_{ov}^2 is flux-pinning limit of a volume defect of over-dopant level at 0 K. The last Equation came from Eq. (5). Therefore, flux-pinning effects ($W_{\Delta H=\Delta B(T),ov}$) superconductor at over-dopant level decrease dramatically as temperature increases compared with those of optimal dopant level.

It is expected that M-H curves of over-doped specimens would be much poorer than those of optimal and less-doped specimen as temperature increases. Figure 3 shows those behaviors, which are that the segregation effects support that M-H curve of the 25 wt.% doped specimen showed poorer M-H curve than that of pure specimen at 30 K although the M-H curve of 25 wt.% doped specimen showed better M-H curve than that of pure specimen at 5 K.

D. Discussion

We suggested that M-H curves of real superconductors have to be considered as three discrete regions owing to their different causes for the regions as shown Fig. 2 (b). If there were no defects in a superconductor, which means no flux-pinning effect, the M-H curve would reduce to ideal superconductor by no increasing diamagnetic property in Region I and deleting $\Delta H=\Delta B$ region, which is Region II. And M-H curve become three regions if volume defects are many enough as being explained. When planar defects are dominant in a superconductor, presence of Region II depends on the dominance of planar defects. Region II completely disappears when dominance of planar defects are high, such as HTSC bulks which were made by solid state reaction method because flux quanta move fast along grain boundaries although they have flux-pinning effects [19, 20].

However, Region II partially appears in the state that dominance of planar defects is low such as water-quenched MgB_2 specimen [21]. In addition, volume defects do not only increase diamagnetic property of the superconductor, but also form Region II. The behavior means that H_{c2} state partially appears in Region II by pinned fluxes at volume defects. The behavior is based on the fact that pinned fluxes at volume defects are pick-out depinned from the defect when the shortest distance between pinned fluxes is the same as that at H_{c2} [2].

Region III is the region that flux-pinning effects of the volume defects are weakened as mentioned. Figure 5 (a) and (b) shows examples of the behavior. They show diamagnetic

properties of 5 wt.% and 10 wt.% (Fe, Ti)-doped MgB₂ along applied magnetic field at various temperatures, respectively. Generally, the better flux-pinning state of the volume defects are, the wider $\Delta H = \Delta B$ region is formed in Region II [2]. Thus, the specimens have shown that wider $\Delta H = \Delta B$ region induced smaller decreases of diamagnetic properties in Region III as applied magnetic field increases. Therefore, it is determined that Region III also affected by flux-pinning effects of volume defects.

The represented theory is only applicable to volume defects-dominating superconductor. All of bulk superconductors except single crystal have grains, which results in making grain boundaries. The air-cooled specimens of current experiment have also grains, thus they have grain boundaries of MgB₂. Nevertheless, the flux-pinning effects of grain boundaries are ignored at low field, which is less than 2 T. It was because effect of volume defects are not only dominant at the field but also the width of grain boundary was short and amount of grain boundaries are small due to large grain size [21].

III. CONCLUSION

We studied flux-pinning effects of (Fe, Ti) particle-doped MgB₂ specimens according to dopant levels of (Fe, Ti) particles, of which radius is 163 nm on average. M-H curves of the specimens are able to be explained as three discreet regions, which are diamagnetic increase region after H_{c1} (Region I), $\Delta H = \Delta B$ region (Region II), and diamagnetic decrease region (Region III). Flux-pinning effect of volume defects-doped superconductor was modeled in an ideal state that the amount of doped volume defects are varied from the optimal dopant level. We focused a width of $\Delta H = \Delta B$ region in comparing theoretical values with experimental results because a degree of diamagnetic decrease is inversely proportional to a width of $\Delta H = \Delta B$ region and max-diamagnetic properties of the doped specimens were almost same.

Results of experiments represented that 5 wt.% (Fe, Ti)-doped MgB₂ showed widest $\Delta H = \Delta B$ region and smallest diamagnetic decrease in diamagnetic decrease region among doped specimens, and widths of $\Delta H = \Delta B$ region gradually became shorter as dopant level increases or decreases from 5 wt.%. In addition, widths of $\Delta H = \Delta B$ region became much shorter as temperature increases as dopant level increased. Comparing experimental results with theory, the two well matched at less-dopant level than optimal dopant level, but the difference between the two increased as dopant level increased from optimal dopant level.

Inspecting the cause that over-doping of (Fe, Ti) particles would reduce flux-pinning effects, it was revealed that flux-pinning limit of a volume defect decreases as dopant level increases, and the segregation effect.

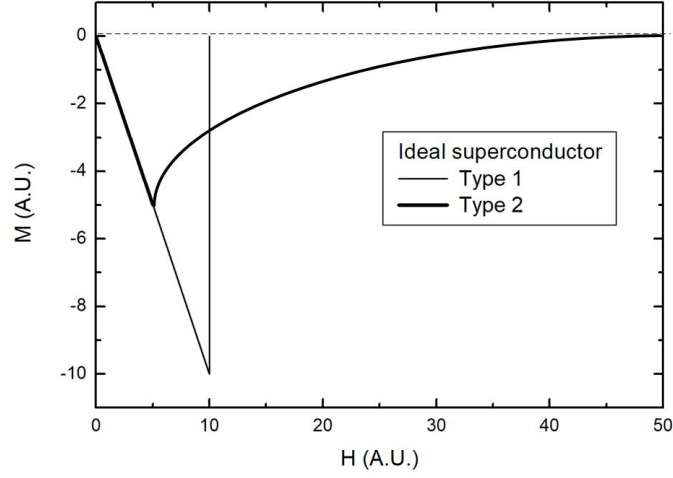
IV. METHOD

(Fe, Ti) particle-doped MgB₂ specimens were synthesized using the non-special atmosphere synthesis (NAS) method [22]. The starting materials were Mg (99.9% powder) and B (96.6% amorphous powder) and (Fe, Ti) particles. Mixed Mg and B stoichiometry, and (Fe, Ti) particles were added by weight. They were finely ground and pressed into 10 mm diameter pellets. (Fe, Ti) particles were ball-milled for several days, and average radius of (Fe, Ti) particles was about 0.163 μm . On the other hand, an 8 m-long stainless- steel (304) tube was cut into 10 cm pieces. One side of the 10 cm-long tube was forged and welded. The pellets and excess Mg were placed in the stainless-steel tube. The pellets were annealed at 300 °C for 1 hour to make them hard before inserting them into the stainless-steel tube. The other side of the stainless-steel tube was also forged. High-purity Ar gas was put into the stainless-steel tube, and which was then welded. Specimens had been synthesized at 920 °C for 1 hour and cooled in air. Field dependences of magnetization were measured using a MPMS-7 (Quantum Design). During the measurement, sweeping rates of all specimens were made equal for the same flux-penetrating condition.

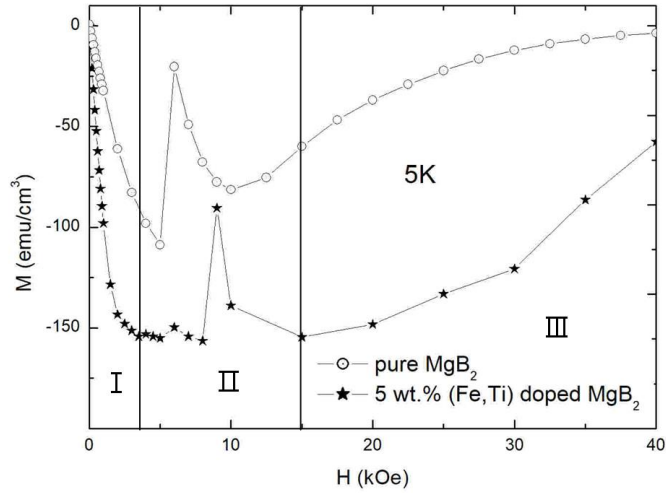
-
- [1] H. B. Lee, G. C. Kim, Y. C. Kim and D. Ahmad, Flux jump behaviors and mechanism of FeTi doped MgB₂ at 5 K, *Physica C* **515** 31 (2015).
 - [2] H. B. Lee, G. C. Kim, H. J. Park, D. Ahmad, and Y. C. Kim, $\Delta H = \Delta B$ Region in Volume Defect-Dominating Superconductors. <https://arxiv.org/abs/1805.04683> (2018).
 - [3] H. B. Lee, G. C. Kim, Y. C. Kim, R. K. Ko, and D. Y. Jeong, Equation of Motion for Pinned Fluxes at Volume Defects and Increases of a Diamagnetic Property by Flux Pinning in Superconductors, <https://arxiv.org/abs/1904.06434> (2019).

- [4] N.S. Kia, S.R. Ghorbani, H. Arabi, M.S.A. Hossain, Effect of magnetic field on the flux pinning mechanisms in Al and SiC co-doped MgB₂ superconductor, *Solid State Communications* **275** 48–52 (2018).
- [5] T. Nishio, Y. Itoh, F. Ogasawara, M. Suganuma, Y. Yamada, U. Mizutani, Superconducting and mechanical properties of YBCO-Ag composite superconductors, *J. of Material Science* **24** 3228–3234 (1989).
- [6] E Martinez, R Navarro and J M Andres, Improvement of the critical current density on in situ PIT processed Fe/MgB₂ wires by oleic acid addition, *Supercond. Sci. Technol* **26** 125017 (2013).
- [7] Sudesh, N Kumar, S Das, C Bernhard and G D Varma, Effect of graphene oxide doping on superconducting properties of bulk MgB₂, *Supercond. Sci. Technol* **26** 095008 (2013).
- [8] Shaopu Tang et al. Improved Transport J_c in MgB₂ Tapes by Graphene Doping, *J Supercond Nov Magn* **27** 2699–2705 (2014).
- [9] Michael Tinkham, *INTRODUCTION TO SUPERCONDUCTIVITY second edition*, Dover Publication, New York 118 (2004).
- [10] Charles P. Poole, Jr., Horacio A. Farach, Richard J. Creswick, *SUPERCONDUCTIVITY 1st* 270, Academic Press.
- [11] A Nabialek et al. The influence of crystal anisotropy on the critical state stability and flux jump dynamics of a single crystal of La_{1.85}Sr_{0.15}CuO₄. *Supercond. Sci. Technol.* **25** 035005 (2012).
- [12] S. Khene, B. Barbara, Flux jumps in YBa₂Cu₃O₇ single crystals at low temperature and fields up to 11 T, *Solid State Communications* **109** 727 (1999).
- [13] Ruixing Liang et al. Growth and properties of superconducting YBCO single crystals. *Physica C* **195** 51 (1992).
- [14] J. C. L. Chow and P. C. W. Fung, Fabrication of Melt-Texture Growth YBCO Samples Using a Simple Muffle Furnace. *J. of Superconductivity* **6** 365 (1993).
- [15] Y. Radzyner et al. Anisotropic order-disorder vortex transition in La_{2-x}A_xSr_xCuO₄. *Phys. Rev. B* **65** 214525 (2002)
- [16] M. Daeumling, J. M. Seuntjens and D. C. Larbalestier, Oxygen-defect flux pinning, anomalous magnetization and intra-grain granularity in YB₂Cu₃O_{7-δ}. *Nature* **346** 332 (1990).
- [17] H. B. Lee, G. C. Kim, Byeong-Joo Kim, and Y. C. Kim, Upper Critical Field Based on the

- Width of $\Delta H = \Delta B$ region in a Superconductor. *Scientific Reports* **10** 5416 (2020).
- [18] H. B. Lee, G. C. Kim, and Y. C. Kim, Temperature Dependence of a Width of $\Delta H = \Delta B$ Region in 5 wt.% (Fe, Ti) Particle-Doped MgB_2 Superconductor <https://arxiv.org/abs/1907.03905> (2019)
- [19] S. Senoussi, M. Oussena, and S. Hadjoud, On the critical fields and current densities of $YB_2Cu_3O_7$ and $La_{1.15}Sr_{0.15}CuO_4$ superconductors, *J. Appl. Phys.* **63** 4176-4178 (1988).
- [20] H M Seyoum et al. Superconducting properties of $Bi_{2-x-y}Pb_xSn_ySr_2Ca_2Cu_3O_z$, *Supercond. Sci. Technol* **3** 616-621 (1990).
- [21] H. B. Lee, G. C. Kim, Hyoungjeen Jeon, Y. C. Kim, Flux-Pinning Effects and Mechanism of Water-Quenched 5 wt.% (Fe, Ti) ParticleDoped MgB_2 Superconductor, *J Supercond Nov Magn* **33** 3673-3679 (2020).
- [22] H. B. Lee, Y. C. Kim and D. Y. Jeong, Non-special atmosphere synthesis for MgB_2 . *J. Kor. Phys. Soc.* **48** 279-282 (2006).

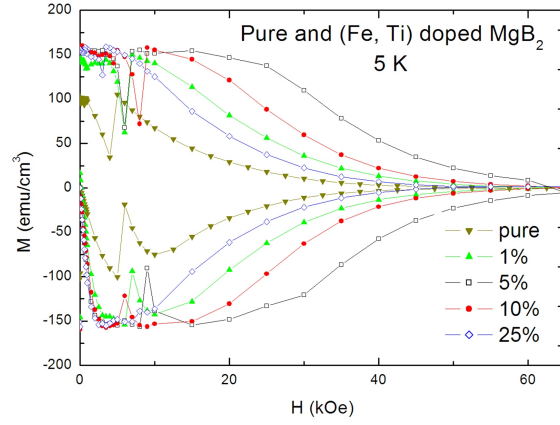


(a)

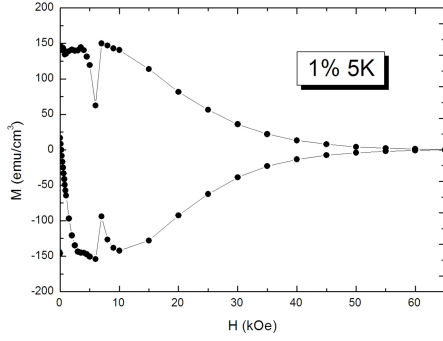


(b)

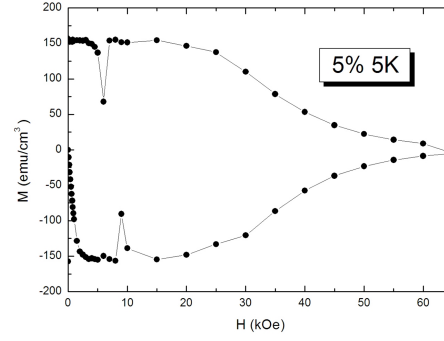
FIG. 1: Field dependences of magnetizations (M - H curves) of superconductors (a): M - H curves of ideal type I and type II superconductors (b): M - H curve of 5 wt.% (Fe, Ti) particle-doped MgB_2 at 5 K, which is volume defect-dominating superconductor. It can be divided as three discrete regions, which are diamagnetic increase region (Region I), $\Delta H = \Delta B$ region (Region II), diamagnetic decrease region (Region III). M - H curve of pure MgB_2 at 5 K is used as a reference.



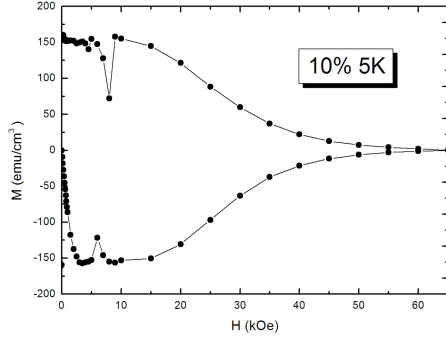
(a)



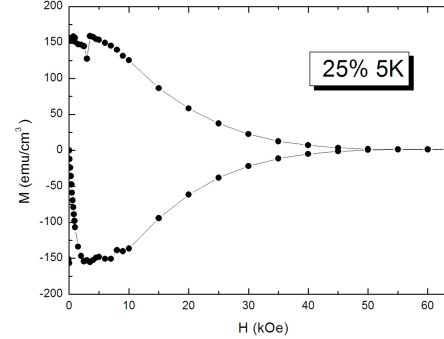
(b)



(c)



(d)



(e)

FIG. 2: Field dependences of magnetizations (M - H curves) at 5 K of wt.% (Fe, Ti) particle-doped MgB_2 specimens, which was air-cooled. (a): M - H curves for comparison. (b): M - H curve of 1 wt.% (Fe, Ti) particle-doped MgB_2 . (c): M - H curve of 5 wt.% (Fe, Ti) particle-doped MgB_2 . (d): M - H curve of 10 wt.% (Fe, Ti) particle-doped MgB_2 . (e): M - H curve of 25 wt.% (Fe, Ti) particle-doped MgB_2 .

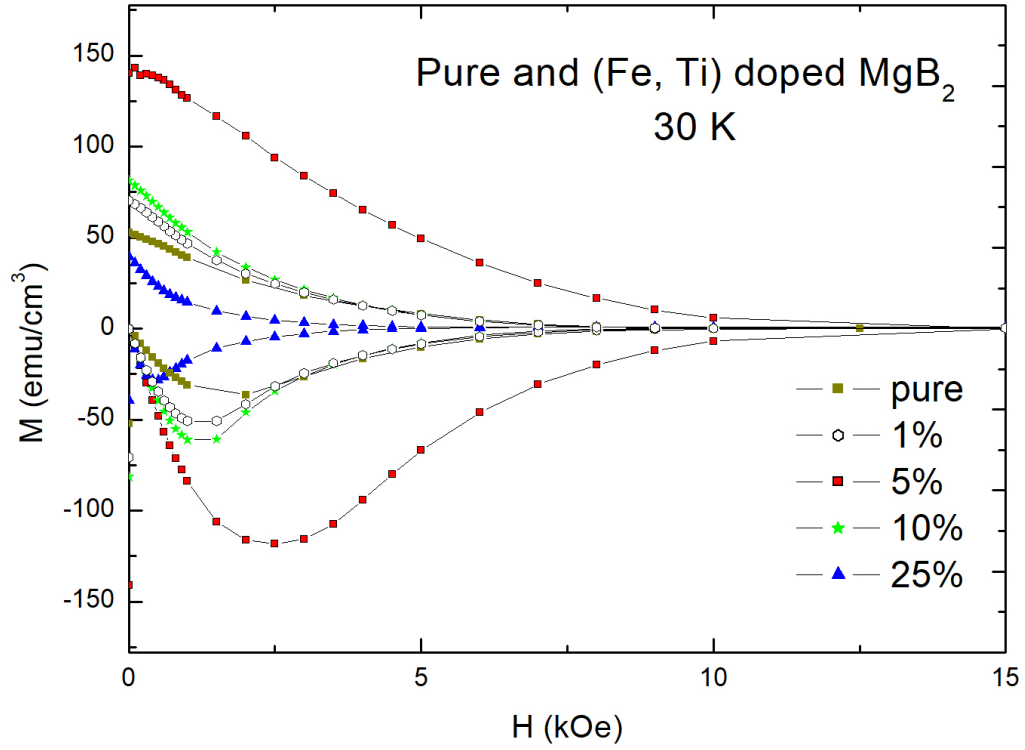
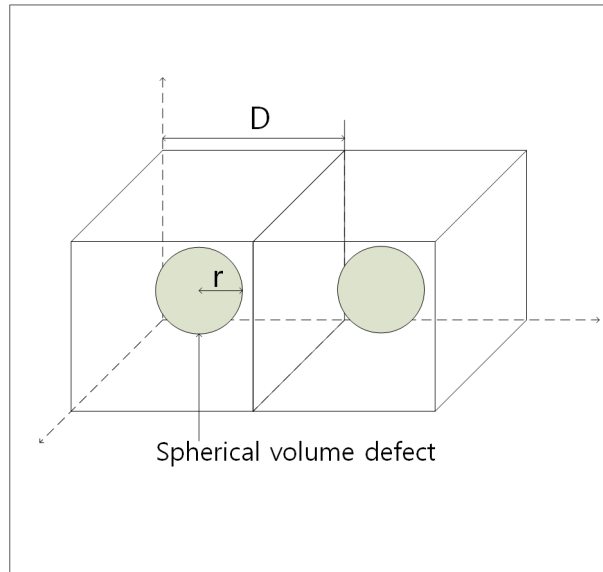
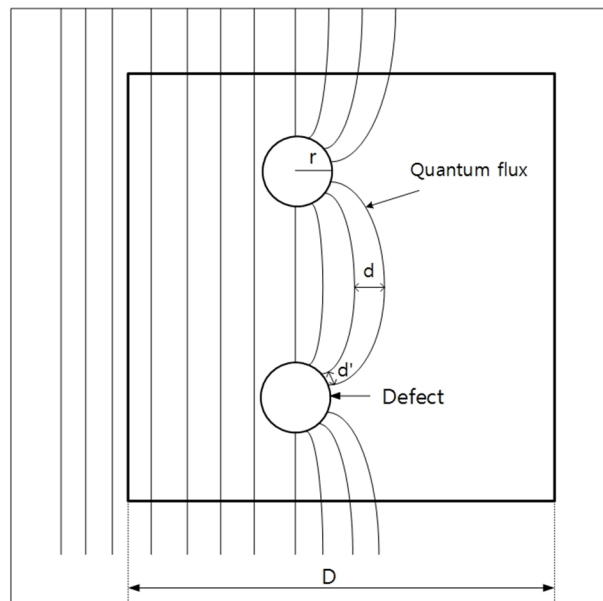


FIG. 3: Field dependence of magnetizations (M-H curves) of wt.% (Fe, Ti) particle-doped MgB₂ at 30 K, which was air-cooled.

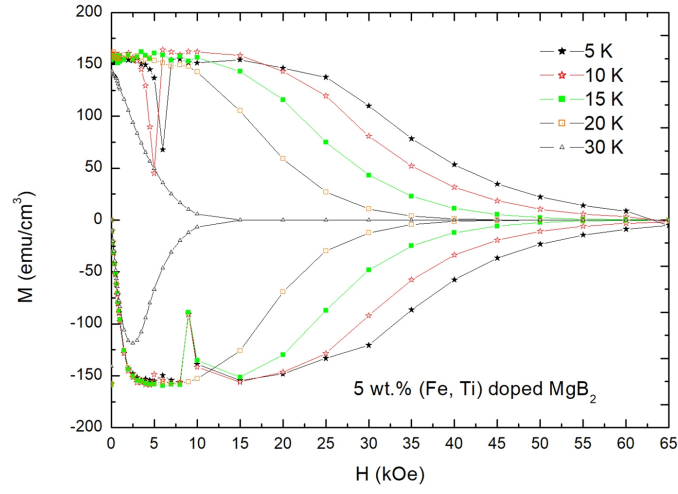


(a)

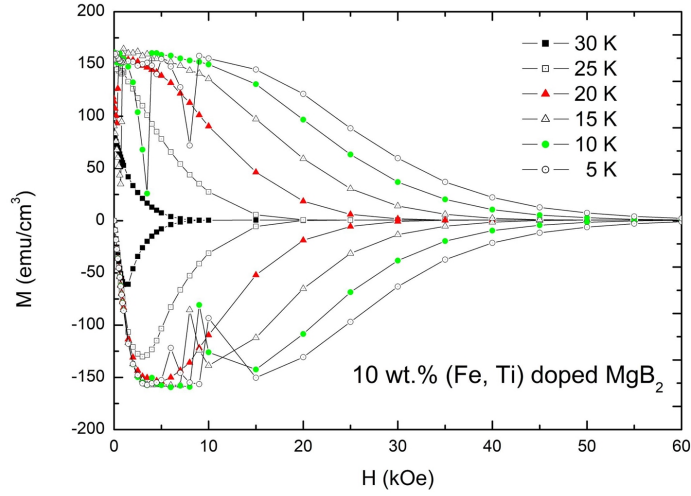


(b)

FIG. 4: (a): Schematic representation of doped volume defects in MgB_2 base. (b): Schematic representation of pinned fluxes at volume defects.



(a)



(b)

FIG. 5: (a): M-H curves of 5 wt.% (Fe, Ti) particle-doped MgB₂ with variation of temperature.

(b): M-H curves of 10 wt.% (Fe, Ti) particle-doped MgB₂ with variation of temperature.

TABLE I: Various properties of (Fe, Ti) doped MgB₂ superconductors according to weight percentage of (Fe, Ti) particles, of which average radius is 163 nm. L' and L are the distance between defects in ideal state and closed packed state, respectively. Closed packed state of volume defects is the state that all of fluxes penetrated are pinned at volume defects ($2r \times m_{cps}=1$, where m_{cps} is the number of volume defects in close packed state [2]). Widths of $\Delta H=\Delta B$ region of specimens are compared with that of 5 wt.% (Fe, Ti) doped MgB₂ as a unit.

Weight percentage	1	5	10	25
Volume percentage	0.4	2	4	10
The number of volume defects in cm ³	4680 ³	8000 ³	10080 ³	13680 ³
The distance (L', r=0.163 μm) between volume defect (Ideal state, μm)	10.15r	5.94r	4.71r	3.47r
The distance (L) between volume defect (Closed packed state, μm)	14.0	4.79	3.02	1.64
Calculated flux-pinning effects (Width of $\Delta H=\Delta B$ region)	0.37	1	0.91	0.75
Experimental results (Width of $\Delta H=\Delta B$ region)	0.4	1	0.67	0.33
Differences between the calculated and experimental results	0.03	0	0.24	0.42
Flux-pinning limit of a volume defect	51 ²	51 ²	38 ²	26 ²